The final publication is available at

https://doi.org/10.1016/j.chemosphere.2017.09.134

Additional Information

1 **Reaction kinetics and mechanisms of organosilicon fungicide flusilazole**

2 **with sulfate and hydroxyl radicals**

3 D. Fabio Mercado[a], Larisa L.B. Bracco[a], Antonio Arques[b], Mónica C. Gonzalez[a], Paula

4 Caregnato[a*]

5 [a]Instituto de Investigaciones Fisicoquímicas Teóricas y Aplicadas (INIFTA), CCT-La Plata-

6 CONICET, Universidad Nacional de La Plata, Casilla de Correo 16, Sucursal 4, (1900) La Plata,

7 Argentina.

8 [b]Grupo de Procesos de Oxidación Avanzada, Departamento de Ingeniería Textil y Papelera,

9 Universitat Politècnica de València, Campus de Alcoy, Plaza Ferrandiz y Carbonell s/n, 03801 Alcoy,

10 Spain.

11

12 *Corresponding author E-mail address: caregnato@inifta.unlp.edu.ar. Postal address: Casilla

13 de Correo 16, Sucursal 4, (1900) La Plata, Argentina.

14

15

16

17 **Abstract**

18 Flusilazole is an organosilane fungicide used for treatments in agriculture and horticulture

19 for control of diseases. The reaction kinetics and mechanism of flusilazole with sulfate and

20 hydroxyl radicals were studied. The rate constant of the radicals with the fungicide were

21 determined by laser flash photolysis of peroxodisulfate and hydrogen peroxide. The results

22 were 2.0×10^9 s^{-1}M^{-1} for the reaction of the fungicide with HO$^\bullet$ and 4.6×10^8 s^{-1} M^{-1} for the

23 same reaction with SO$_4^{\bullet-}$ radicals. The absorption spectra of organic intermediates detected

24   by laser flash photolysis of $S_2O_8^{2-}$ with flusilazole, were identified as α-aminoalkyl and

25   siloxyl radicals and agree very well with those estimated employing the time-dependent

26   density functional theory with explicit account for bulk solvent effects. In the continuous

27   photolysis experiments, performed by photo-Fenton reaction of the fungicide, the main

28   degradation products were: (bis(4-fluorophenyl)-hydroxy-methylsilane) and the non-toxic

29   silicic acid, diethyl bis(trimethylsilyl) ester, in ten and twenty minutes of reaction,

30   respectively.

31

32   Keywords: flusilazole, fungicide degradation, degradation mechanism, sulfate radical,

33   hydroxyl radical, photo-Fenton.

34

35

Introduction

Advanced oxidation processes (AOPs), like UV/ $S_2O_8^{2-}$ and Fenton, have attracted interest for the degradation of organic compounds in wastewater, such as pesticides (Carra et al. 2016)(Navarro et al. 2011). This is especially true in the case of the use of light-induced reactions in water treatments. The photo-assisted Fenton reaction ("photo-Fenton" reaction) typically gives faster rates and a higher degree of mineralization than the thermal reaction and can take the advantage of light in the solar spectral region (Faust and Hoigné 1990). In photo-Fenton process Fe^{2+} ions are oxidized by H_2O_2 and one equivalent $HO^{\bullet}$ is produced. The obtained $Fe(OH)^{2+}$, which is predominant in acidic conditions, act as the light absorbing species that produce another radical while the initial Fe^{2+} is regained (Kim and Vogelpohl 1998). Persulfate reaction mechanism is based on the generation of the strong sulfate radical ($SO_4^{\bullet-}$). One mole of this reagent can be activated to generate two moles of sulfate radical under UV irradiation. The sulfate radical is known to be a very strong oxidant, i.e. E ($SO_4^{\bullet-}$/ SO_4^{2-}) = 2.43 V vs. NHE (Criquet and Leitner 2009) for degrading organic contaminants in wastewater (Wang and Liang 2014) (Luo et al. 2017).

Flusilazole is the approved name for 1-[[bis(4-fluorophenyl)methyl]silyl]methyl]-1H-1,2,4-triazole (CAS No. 85509-19-9). It is a triazole family fungicide with a molecular structure shown in scheme 1. It is a broad-spectrum fungicide, which exhibits curative and preventative activities and is recommended for use in agriculture and horticulture (T. R. Roberts and Hutson 1990).
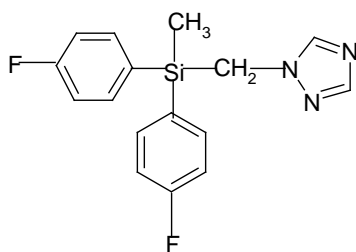
57

58   Scheme 1. Flusilazole

59

60   Pesticides can easily accumulate in plants, foods, water reservoirs and food chain, which

61   could be triggered by indiscriminate use. Besides, some of them are resistant to the action of

62   sunlight, temperature, water or microorganisms; as a result of this, plant tissue and

63   environmental samples contain high levels of pesticides residues.

64

65   It was suggested that flusilazole is capable of inducing genotoxicity in plants in studies with

66   higher plant models (Ozakca and Silah 2013). Animal models in vitro and in vivo have been

67   used to investigate the teratogenecity of flusilazole. Some studies reported marked maternal

68   toxicity, growth retardation, and skeletal in rodent models, which contribute to alterations in

69   fetal growth retardation and skeletal development (Farag and Ibrahim 2007). Besides

70   embryotoxic responses are critically dependent on the timing of exposure during rat embryo

71   development (Dimopoulou et al. 2016).

72   Photolysis (artificial and natural sunlight) on soil surface and aqueous photodegradation is

73   not an important mode of degradation for flusilazole (T. R. Roberts and Hutson 1990).

74   Despite flusilazole is a widely used fungicide, documented data on their degradation

75   mechanism and intermediate metabolites is lacking. Differences in chemical reactivity

76   between silicon and carbon compounds influence the degradation and oxidative metabolism

77   of otherwise similar compounds. For instance, organic silicon compounds usually lead to

78 naturally occurring silicates as final product, in sharp contrast with the carbon containing

79 analogous compounds (Griessbach and Lehmann 1999).

80

81 In this context, the aim of the present work is to investigate the kinetics and mechanism of

82 the degradation of flusilazole initialed by $HO^{\bullet}$ and $SO_4^{\bullet-}$. These radicals have been generated

83 by laser flash photolysis ($\lambda_{exc.}$=266nm) of H_2O_2 and $Na_2S_2O_8$, respectively. Also, continuous-

84 irradiation experiments have been performed by photo Fenton reaction of the fungicide and

85 the nature of the primary degradation products formed have been investigated by GC-MS

86 analysis.

87

88 **Experimental**

89 *Reagents.* Flusilazole (1-((bis(4-fluorophenyl)methylsilyl)methyl)-1H-1,2,4-triazole), was

90 purchased from Sigma-Aldrich (Fluka). Sodium peroxodisulfate was obtained from Merck.

91 Ferrous chloride tetrahydrate ($FeCl_2 \cdot 4H_2O$) 98% was obtained from Fisher Chemical. H_2O_2

92 30%(w/w) in H_2O was supplied by Sigma-Aldrich. Potassium thiocyanate was from

93 Mallinckrodt.

94 Distilled water was passed through a Millipore system (>18 MX cm, <20 ppb of organic

95 carbon).

96

97 *Sample Preparation.* Flusilazole (F) saturated aqueous solution was prepared to set up

98 suspensions of lower concentrations by dilution. Oxygen-free and oxygen saturated solutions

99 were obtained by bubbling the samples with argon or oxygen, respectively, for 20–30 minutes

100 before use.

101   In continuous photolysis experiments the pH of the solution was adjusted to 3.0 using HCl

102   and the sample was mixed using a magnetic stirrer during the process.

103

104   *Laser Flash Photolysis (LFP) Experiments.* LFP experiments were performed by excitation

105   with the fourth harmonic of a Nd:YAG Litron laser (2 ns fwhm, 2 mJ per pulse at 266 nm).

106   The analyzing light from a 350 W Xe arc lamp was passed through a monochromator (PTI

107   1695) and detected by a 1P28 PTM photomultiplier. Due to the characteristics LFP detection

108   system used, traces with $\lambda>650$nm and $\lambda<290$nm could not be detected within the

109   experimental error. A cuvette of 10 mm path length was used for the sample container.

110   Decays typically represented the average of 32 laser shots and were stored in a 500 MHz

111   Siglent digital oscilloscope. Solution absorbance was 0.5 at 266 nm. Reactant concentrations

112   were: $[Na_2S_2O_8] = 1.0$–2.5×10^{-2} M and flusilazole was in the range 8.49×10^{6} M – 8.50×10^{-5}

113   M.

114   Freshly prepared solutions were used in order to avoid thermal reactions of peroxodisulfate

115   and hydrogen peroxide with the substrate.

116   *Bilinear regression analysis*. For each experimental condition, several absorbance decay

117   profiles at different detection wavelengths were taken. Absorbance is thus a function of

118   wavelength and time. Taking advantage of the linearity of the absorbance with both,

119   concentrations and absorption coefficients, a bilinear regression analysis was applied to the

120   experimental absorption matrix in order to retrieve information on the minimum number of

121   species and on their relative concentration profiles and absorption spectra [San Román and

122   Gonzalez, 1989].

123 *Time-dependent density functional theory calculations.* Time dependent density functional

124 calculations, TD-DFT, has been employed in numerous studies as a useful tool to characterize

125 electronically excited states of a large number of molecules (Dell 'Arciprete et al. 2011)

126 (Arce et al. 2012). In this work, the hybrid B98 (Schmider and Becke 1998) density

127 functional combined with the 6-311++G(d,p) basis set, was used to interpret the spectra of

128 the observed transient species. To account for solvent effects, the conductor-like polarizable

129 continuum model, CPCM, was employed using a relative permittivity for H_2O of 78.3553

130 (Barone and Cossi 2001). In this way, the interaction between solvent and solute molecules

131 was considered. All calculations have been carried out with the Gaussian 09 package (Frisch

132 et al. 2009). To obtain the theoretical absorption spectrum it is firstly necessary a full

133 optimization of the geometric parameters of the considered ground-state molecule. In all the

134 cases, real frequencies were obtained indicating that molecular structures correspond to

135 stable species. Next, the vertical electronic energies, the associated wavelengths of the band

136 maxima, λ_{max}, and oscillator strengths *f* were computed at the abovementioned level of

137 theory.

138 To compare the prediction with experimental data, theoretical bands were approached with

139 individual Gaussian functions characterized with full width values σ (at the 1/e height of the

140 bands) and summed over all relevant electronic transitions (Cobos and Croce 2010). As

141 Figure 3 shows, a satisfactory agreement between the experimental and the modeled spectra

142 for all species are obtained using a standard value of σ = 0.21 eV.

143

144 *Chemical analysis*

145 The concentration of flusilazole was determined by HPLC and reaction products of fenton

146 reactions were analyzed by GC-MS.

147   Samples were irradiated in a cylindrical glass reactor with a solar simulator (Oriel

148   Instruments, Model 81160) equipped with a 300W xenon lamp and a cut off 300nm filter.

149   The prepared solution was 5ppm of Fe^{2+} and 1.23×10^{-3} M of flusilazole. 50µL of H_2O_2 was

150   added to a volume of 250mL.

151   **HPLC analysis**. In order to follow the concentration of the flusilazole in the reaction system,

152   a Merck Hitachi XL Autosystem D-7000 chromatograph with a diode array detector was

153   used. The column used to separate the flusilazole was a LiChroCART® 125-4 with reverse

154   phase LiChrospher® 100 RP-18 (5µm) from Merck. Samples of 0.5 mL were directly taken

155   from the reaction system and they were diluted with 0.5 mL of methanol. The injection

156   volume was 80 µL. As mobile phase a mixture of water:methanol (20:80) (v/v) were used in

157   a flow 0.8 mL min-1. The detection wavelength was 230 nm and the retention time for the

158   flusilazole was about 5.1 minutes.

159   **GC-MS**. After selected periods of irradiation (10 or 20 minutes) , the reactor was emptied

160   and the treated solution was concentrated by means of solid phase extraction: 100 mL of the

161   aqueous solution were flown though a LiChrolut EN 200 mg (Merck) cartridge and the

162   adsorbed organics were recovered with 3 mL of methanol. A GCMS-QP2010S (Shimadzu)

163   gas chromatograph equipped with a quadrupole mass analyzer was employed to identify

164   major intermediates formed along the process. The temperature program for GC analysis

165   involved a heating method with a constant ramp from 60ºC to 250ºC at a rate of 5ºC/min rate.

166   A Meta X5 Teknokroma column was used. The retention time for the flusilazole and the

167   observed products are listed in the table 1.

168

169 **Results and discussion**

170 **Experiments with HO• radicals**

171 *Continuous photolysis experiments*

172 Irradiation of 1.23×10^{-3}M aqueous solutions of flusilazole with the solar simulator, shows

173 depletion of the fungicide with the photolysis time. According to Figure 1, five minutes of

174 irradiation were needed to achieve 80% abatement of flusilazole in the presence of 5 ppm

175 Fe^{2+} and 50 µL of H_2O_2 at pH=3.
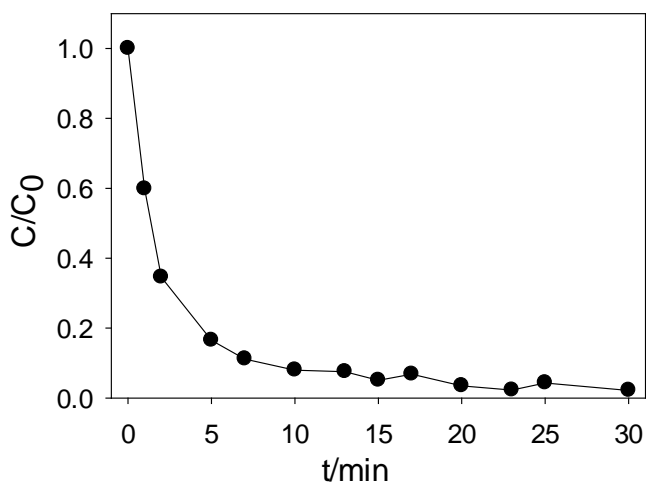
176

177 **Figure 1**. Fungicide depletion (1.23×10^{-3} M) in photolysis experiments with light of solar

178 simulator at pH=3.

179

180 *Stable products identification*

181 Aqueous solutions containing Fe^{2+}, H_2O_2, and flusilazole in the concentrations indicated

182 above, were irradiated for 10 and 20 minutes with the solar simulator to detect the

183 degradation products formed after reaction 2.

Table 1 summarizes the GC-MS mass peaks and fragments detected for the degradation
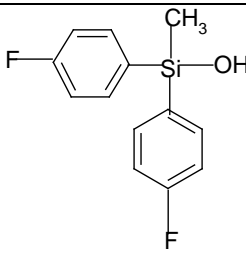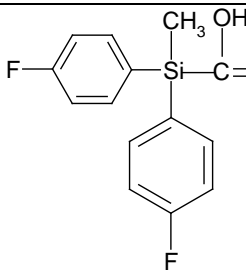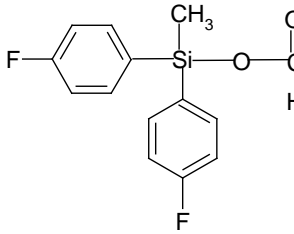
products of the fungicide.

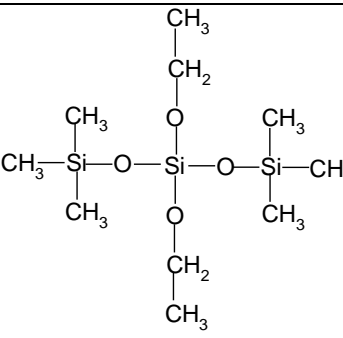|	
$Fe^{2+} + H_2O_2 \longrightarrow Fe(OH)^{2+} + HO^{\bullet}$	1(Trovó et al. 2008)(Kim and Vogelpohl 1998)
$Fe(OH)^{2+} + hv \rightarrow Fe^{2+} + HO^{\bullet}$	
$HO^{\bullet} + F \longrightarrow$	2

Table 1. Degradation products.

Products present after 10 minutes irradiation			
R_t(min)	MW (characteristic ions, m/z)	Product assignment	
19.6	250 (236, 235, 155, 96)		Compound 1 (bis(4-fluorophenyl)-hydroxy-methylsilane) Scheme III
(20.43-20.48)	278 (235, 236, 170, 169, 155, 156, 139, 140, 96, 45)		Compound 2 Scheme IV

			Compound 2´ Scheme III
Products present after 20 minutes reaction			
>28	296(282, 281, 209, 208, 207, 73)		Silicic acid, diethyl bis(trimethylsilyl) ester

After 20 minutes of photo-Fenton reaction with flusilazole, the GC-MS peaks of $R_t < 26.5$ min could not be identified due to the complex reaction system, which lead to a high number of reaction by-products reaching low concentrations.

Kinetic measurements

Hydroxyl radicals (HO•) were generated by LFP of 0.1 M H_2O_2 aqueous solution ($\lambda_{exc.} = 266$ nm), reaction 1´.

$H_2O_2 \xrightarrow{h\nu} HO^\bullet$	1´
$F + HO^\bullet \longrightarrow$	2

200   The rate constant for the reaction of flusilazole with HO$^\bullet$ radicals (reaction 2) was assessed

201   by the competition method $k(\text{F} + \text{HO}^\bullet)= 2.0\times10^9$ s^{-1}M^{-1} (Kozicki et al. 2003) (Dell 'Arciprete

202   et al. 2009) (See Supplementary data). The concentration range of flusilazole solutions used

203   was 0-1.12$\times10^{-4}$ M.

204   A degradation mechanism is proposed for the reaction of hydroxyl radicals and flusilazole.

205   Tertiary amines are reactive sites for HO$^\bullet$ radical attack (Das and von Sonntag 1986) (Dell

206   'Arciprete et al. 2009). The simplest oxidation process for a tertiary amine is single electron

207   transfer from the non-bonding electron pair of the amine to form a radical cation, followed

208   by a α-CH bond cleavage or hydrogen atom transfer. The process will be denoted as

209   hydrogen-atom transfer if the electron and proton aceptor are the same identity

210   (Sumalekshmy and Gopidas 2005) (Suresh Das and V. Suresh 2001).

211   Scheme II show a possible reaction pathway, which involves an initial electron transfer by

212   HO$^\bullet$ radicals to yield a radical cation in the N tertiary atom of triazole ring followed by

213   elimination of H$^+$ ion to yield a more stable α aminoalkylradical.
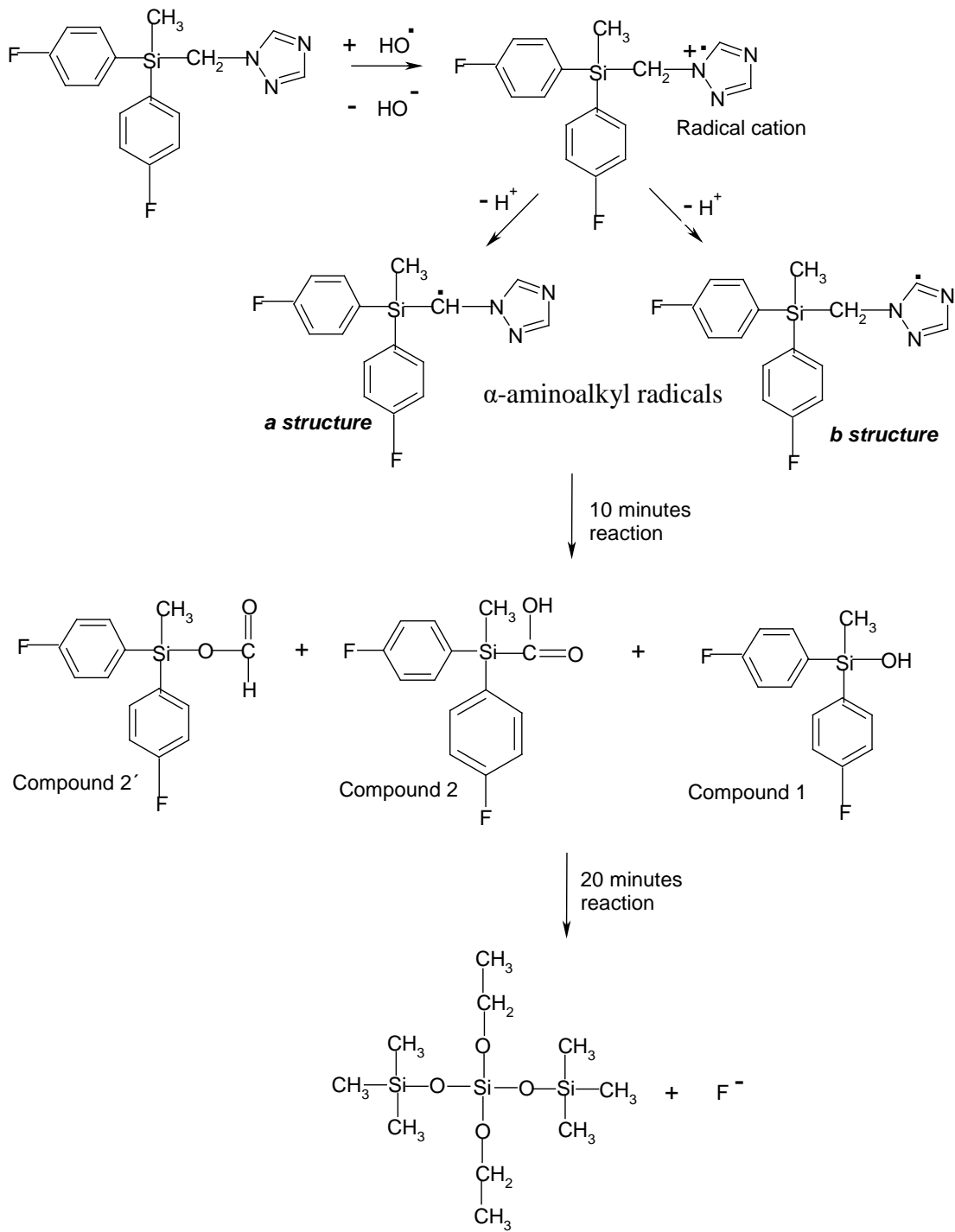
214

215   Scheme II

216

217   **Experiments with SO$_4^{\bullet-}$ radicals**

218

219   It is not possible to detect organic intermediates generated by reaction of hydroxyl radicals

220   with flusilazole using the indirect method. In order to confirm the first steps of the mechanism

221   proposed in scheme II, LFP experiments initiating the oxidation of flusilazole with highly

222   oxidative species such as sulfate radicals (SO$_4^{\bullet-}$) were performed.

223

224   *Kinetic measurements*

225   In LFP experiments of aqueous $1.0 - 2.5 \times 10^{-2}$ M peroxodisulfate solutions, a transient specie

226   was formed in the wavelength range of 330–500 nm (reaction 3). The obtained decay rate

227   and spectrum are in agreement with those reported in the literature for SO$_4^{\bullet-}$ (Choure et al.

228   1997).

229

| $S_2O_8^{-2} \xrightarrow{h\nu} 2SO_4^{\bullet-}$	3
$F + SO_4^{\bullet-} \longrightarrow$	4

230

231   The SO$_4^{\bullet-}$ radical absorbance decay at detection λ (ΔA), fit to equation (1) which shows both

232   first and second–order components (See supplementary data):

233     $$\Delta A = \frac{a}{b(\lambda)\exp(at) - c(\lambda)} \qquad \text{eqn (1)}$$

234   Where: a is the apparent first order decay constant (K_{app}), and $b(\lambda) = (a / \Delta A_0) + c(\lambda)$. The

235   second order constant $2k/\varepsilon(\lambda)$ is calculated from $c(\lambda) = 2k/\varepsilon(\lambda)l$, where $\varepsilon(\lambda)$ is the absorption

236   coefficient at a certain wavelength , and l is the optical path. ΔA_0 is absorbance at t=0.

237 Photolysis experiments of sodium persulfate aqueous solutions in the presence of flusilazole

238 $(4.25 \times 10^{-5}\,M > [F] > 8.47 \times 10^{-5}\,M)$, showed formation of transient species in the wavelength

239 range from 300 to 650 nm. The decay kinetics of the traces observed strongly depend on

240 wavelength. Therefore, a bilinear regression analysis was used to retrieve kinetic and

241 spectroscopic information of the individual species in the reaction mixture.

242 Sulfate radical anion is the only specie that absorbs at $\lambda = 450$ nm. Sulfate radical traces show

243 a first order decay with an apparent rate constant, k_{app}, increasing with flusilazole

244 concentration, as depicted in the inset of figure 2.

245 The slope of the straight line in the figure 2, yields the rate constant k for the reaction of

246 sulfate radicals with flusilazole (reaction 4) $k(F + SO_4^{\bullet-}) = (4.6\pm0.4) \times 10^8\ s^{-1}M^{-1}$.
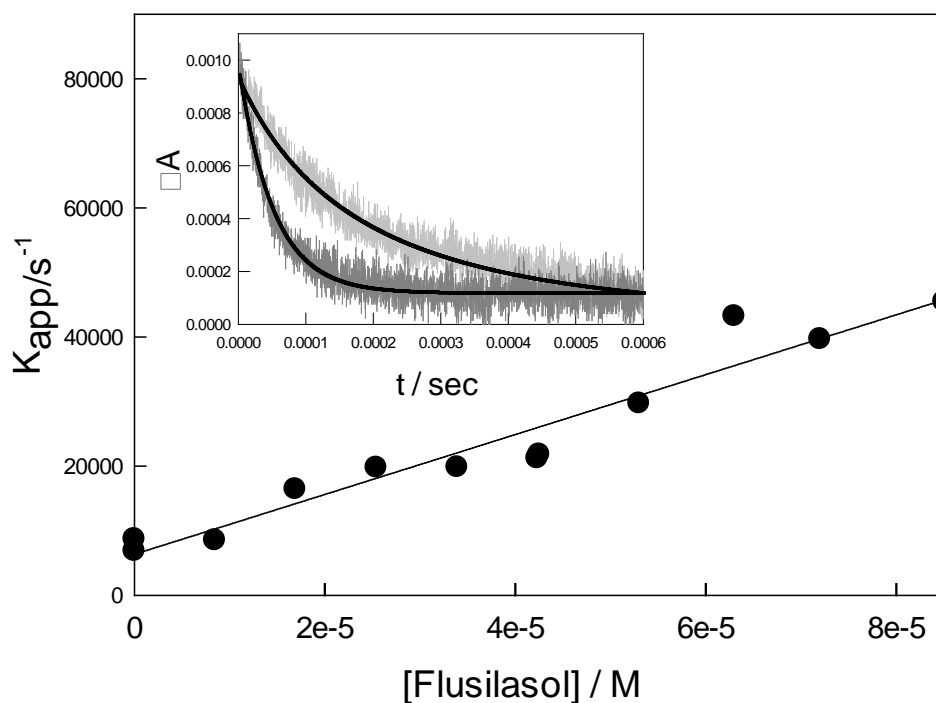
247

248 **Figure 2.** Apparent rate constants, K_{app} vs. [F] obtained in experiments with 2.5×10^{-2} M

249 sodium peroxodisulfate $Na_2S_2O_8$ aqueous solutions. **Inset**: Absorbance profiles at 450nm

250 obtained in experiments with 2.5×10^{-2} M peroxodisulfate $S_2O_8{}^{2-}$ solutions in the presence

251 (dark grey curve) and absence (light grey curve) of 4.25×10^{-5} M of F. The full lines stand

252 for the fittings to eqn (1).

253

254 *Intermediates formed after the reaction of $SO_4{}^{\bullet-}$ radicals with flusilazol.*

255 At high flusilazole concentrations the decay rate of $SO_4{}^{\bullet-}$ radicals becomes too fast to be

256 observed in our time resolution range. On the other hand, laser flash photolysis of flusilazole

257 solutions in the absence of persulfate showed no traces, within our experimental error, in the

258 UV and visible range. Therefore, under these conditions, the observed traces may be assigned

259 to organic transients formed after reaction of $SO_4{}^{\bullet-}$ with flusilazole (reaction 4).

260 To study the spectra and decay rates of the organic intermediates, experiments were

261 performed with solutions containing the highest concentration of flusilazole used (8.47×10^{-5}

262 M) and 2.5×10^{-2} M of persulfate.

263 A bilinear analysis of the absorbance matrix (see Experimental Section above), shows that

264 the system could be described by two absorbing species in the wavelength range from 290 to

265 640 nm, named transient 1 and transient 2. The first transient absorbs at wavelengths of

266 300nm, and the second one has two maxima at 350-360 nm and 640 nm, respectively.

267 In order to gain further insight into the transients' nature, the reaction with molecular oxygen

268 was investigated. To that purpose, LFP experiments under argon, air and oxygen saturated

269 atmosphere with 2.5×10^{-2} M $S_2O_8{}^{2-}$ solutions and 8.47×10^{-5} M of flusilazole were performed.

270 The absorption spectra of the organic transient in the range 300–400 nm (transient 1), were

271 similar in all three cases, within the error of the determination (See Figure S1 at

272 Supplementary data). The decay profiles of this transient fit to a mixed first and second order

16

273 reaction rate law in the presence of oxygen (absorbance traces fit to equation 1). Mainly a

274 second order decay was observed in Ar- saturated solutions (see equation at Supplementary

275 data). The first order decay rate constant was 2.2×10^3 s^{-1} and 3.4×10^3 s^{-1} in air- and oxygen-

276 saturated samples, respectively. The second order component $2k/ \varepsilon_{(300nm)} \sim 6 \times 10^6$ cm s^{-1} was

277 independent on the presence of oxygen. The presence of a second order term in the decay

278 traces might indicate a recombination of transient 1.

279 The second transient had two absorption maxima at 350nm and 640 nm with a decay profile

280 that fits a mixed first and second order equation (eqn 1). No dependence of both first and

281 second order constants with the concentration of dissolved oxygen was observed (see table

282 2). However, the absorbance intensity of the second transient was dependent on the

283 concentration of dissolved oxygen.

284

285 Table 2. First order decay component (*a*) and second order one (*b*) obtained from the fit of

286 decay traces of transient 1 and 2 by eqn (1).

	a	$b = 2k/\varepsilon(\lambda)$
Transient 1 ($\lambda_{max}\sim300$nm)	2.2×10^3 s^{-1}(Air) 3.4×10^3 s^{-1} (bubbling oxygen)	6×10^6 cm s^{-1} (bubbling Ar, air and oxygen)
Transient 2 ($\lambda_{max}\sim350$ and 640nm)	1×10^4 s^{-1} (bubbling Ar, air and oxygen)	1×10^6 cm s^{-1} (bubbling Ar, air and oxygen)

287

288   The one-electron charge transfer reaction from amine nitrogen to sulfate radicals to yield a

289   radical cation in the N atom has been reported (Dell 'Arciprete et al. 2011). On the other

290   hand, the rate constants for the $SO_4^{\bullet-}$ hydrogen-abstraction from C–H bonds were smaller

291   than those measured here for the reactions of sulfate radical with the fungicide (10^5 to 10^7 s$^-$

292   ^{1} M^{-1}) (Neta et al.1988).

293   Nitrogen-centered radical cations do not efficiently react with molecular oxygen, as observed

294   in other organic transients (Bosio et al. 2005) (Dell'arciprete et al. 2007). It is discussed in

295   literature that α-aminoalkyl radicals are formed after the elimination of H$^+$ from nitrogen-

296   centered radical cations; this α-aminoalkyl radicals are highly stabilized by the free electronic

297   pair of the vicinal nitrogen (Padmaja et al. 1993)(Luke et al. 2003)(Ito et al. 2009).

298   Considering that the amine-type nitrogen atom in the triazole moiety of flusilazole present

299   H-atoms α to nitrogen, identification of the observed transients as α-aminoalkyl radicals is

300   strongly suggested. Furthermore, α-aminoalkyl radicals show significant absorbance up to

301   500 nm and react with molecular oxygen (Dell 'Arciprete et al. 2009) (Hiller and Asmus

302   1983) (Lalevée et al. 2007), in agreement with the behavior of the first transient herein

303   observed.

304   The second transient signal grows quickly, reaching its maximum value about 13 μs after the

305   laser shot, and it decays within 500 μs (See Figure S3 at Supplementary data). Besides, its

306   formation depends on the concentration of dissolved oxygen in the sample. This behavior

307   may be explained by a reaction mechanism in which this transient is formed via the reaction

308   of the first transient with oxygen. Peroxyl radicals generated by reaction of α-aminoalkyl

309   radicals with oxygen could lead to the formation of siloxyl radicals, which are assigned to

310   the second transient, as will be discussed later in the manuscript.

311

312   *Reaction pathways*

313   As discussed before, a charge transfer pathway leads to the formation of sulfate anions and

314   the radical cation of flusilazole, which upon elimination of H^+ leads to α-aminoalkyl radical.

315   To help identify the nature of the observed transients, the TD-DFT spectra of α-aminoalkyl

316   radicals in carbon (structures *a* and *b*) and the radical cation were calculated.

317   The coincidence obtained between the experimental first transient spectrum and those

318   calculated for the *a* structure of α-aminoalkyl radicals, indicates that the observed transient

319   may be assigned to the specie where carbon radical lies in the carbon atom vicinal to silicon

320   in flusilazole molecule (figure 3). Radical cation in the N triazole atom is proposed in the

321   first reaction step of scheme II. A reactive intermediate with a TD-DFT spectra absorption

322   bellow 240nm with $\lambda_{max.}$=210nm, was not detectable in the time window of our experimental

323   LFP setup.

324   Calculations for the *b* structure of α-aminoalkyl radical in carbon, shows a spectrum with a

325   low absorption coefficient at 300nm (figure 3).
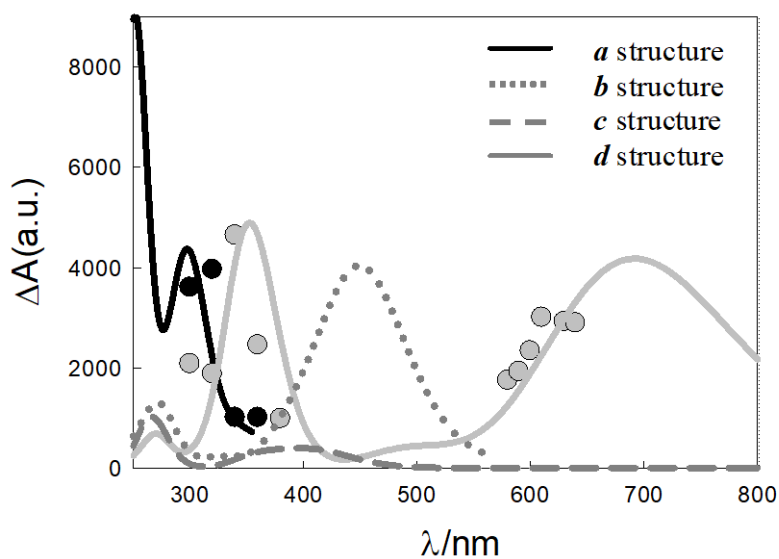
326

327   **Figure 3**. Absorption spectra in arbitrary units of transient 1 (black circles) and transient 2

328   (grey circles) obtained at 1×10^{-5}sec from bilinear analysis of LFP experiments with 2.5×10^{-2}

329   ^{2} M $S_2O_8^{2-}$ and 8.47×10^{-5} M Flusilazole in argon saturated solutions. The full, dotted and

330   dashed lines stand for the calculated TD-DFT spectra.

331

332   The mechanism discussed above strongly confirms that the more reactive group of flusilazole

333   is the triazole ring, as was proposed according to the by-products detected by GC-Mass in

334   photo-Fenton reactions.

335   The α-aminoalkyl radicals ($-HC^{\bullet}-N<$) (Hiller and Asmus 1983) (Baciocchi et al. 2004) may

336   either further react with molecular oxygen to yield peroxyl radicals (*c structure*), or

337   recombine leading to the eventual production of flusilasole-amine dimer (Hasegawa et al.

338   1988) (See Scheme III).
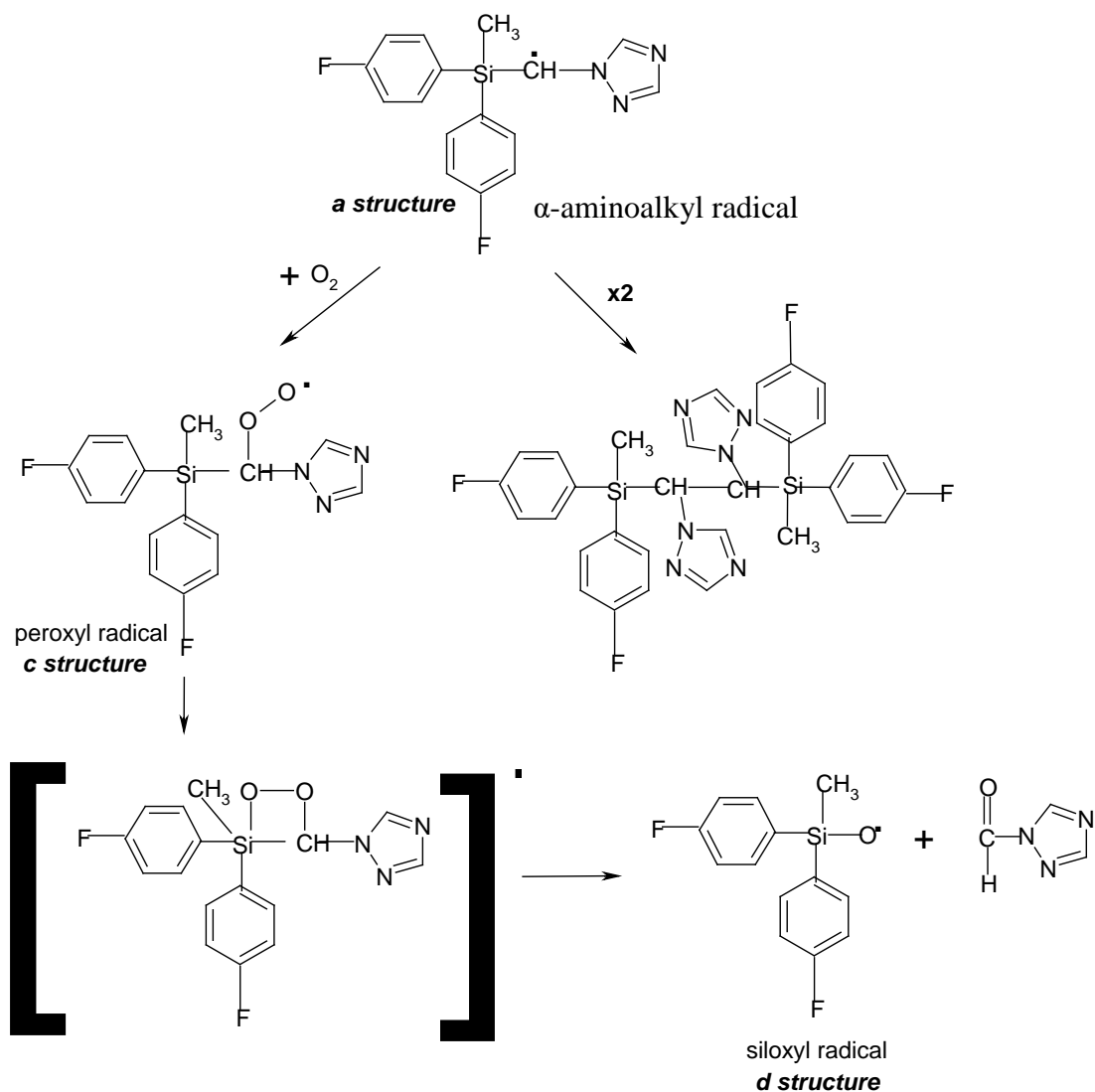
339

340   Scheme III

341

342   Peroxyl radicals (*c structure*) may produce siloxyl radicals through a mechanism that

343   involves silicon pentacoordinated intermediates as shown in Scheme III. A similar

344   mechanism was proposed by Corriu and co-workers for the hydrolysis of tetracoordinate

345   silicates initiated by a nucleofilic attack leading to pentacoordinate silicon intermediate

346   (Corriu et al. 1991).

347 Formation of transient d (d structure) is strongly suggested, due to the high affinity of oxygen

348 to silicon. Si-O$^{\bullet}$ radical could be depleted by reaction with hydrogen peroxide or other

349 hydrogen donor in the media, leading to the formation of silanol.

350 The TD-DFT calculated spectra of peroxyl radical (structure c), has a wavelength maximum

351 around 270 nm, not observed in the experimental conditions of this setup. However, the

352 second transient with $\lambda_{max.}$ at 350 and 640nm, is very similar to the one calculated called d

353 radical which it is also shown in figure 3 and may be assigned to that specie.

354

355 **Reaction of HO$^{\bullet}$ radicals with flusilazol in continuous photolysis experiments. Reaction**

356 **pathways**

357 Based on the detailed reaction mechanism for the first steps of reactions of SO$_4^{\bullet-}$ with

358 flusilazole with identification of organic transients formed, a complete pathway for the initial

359 photochemical products and primary steps of HO$^{\bullet}$ radical oxidation of flusilazole is proposed

360 in Scheme IV y V yielding compound 1, compound 2 and 2´ (GC-MS products)

361
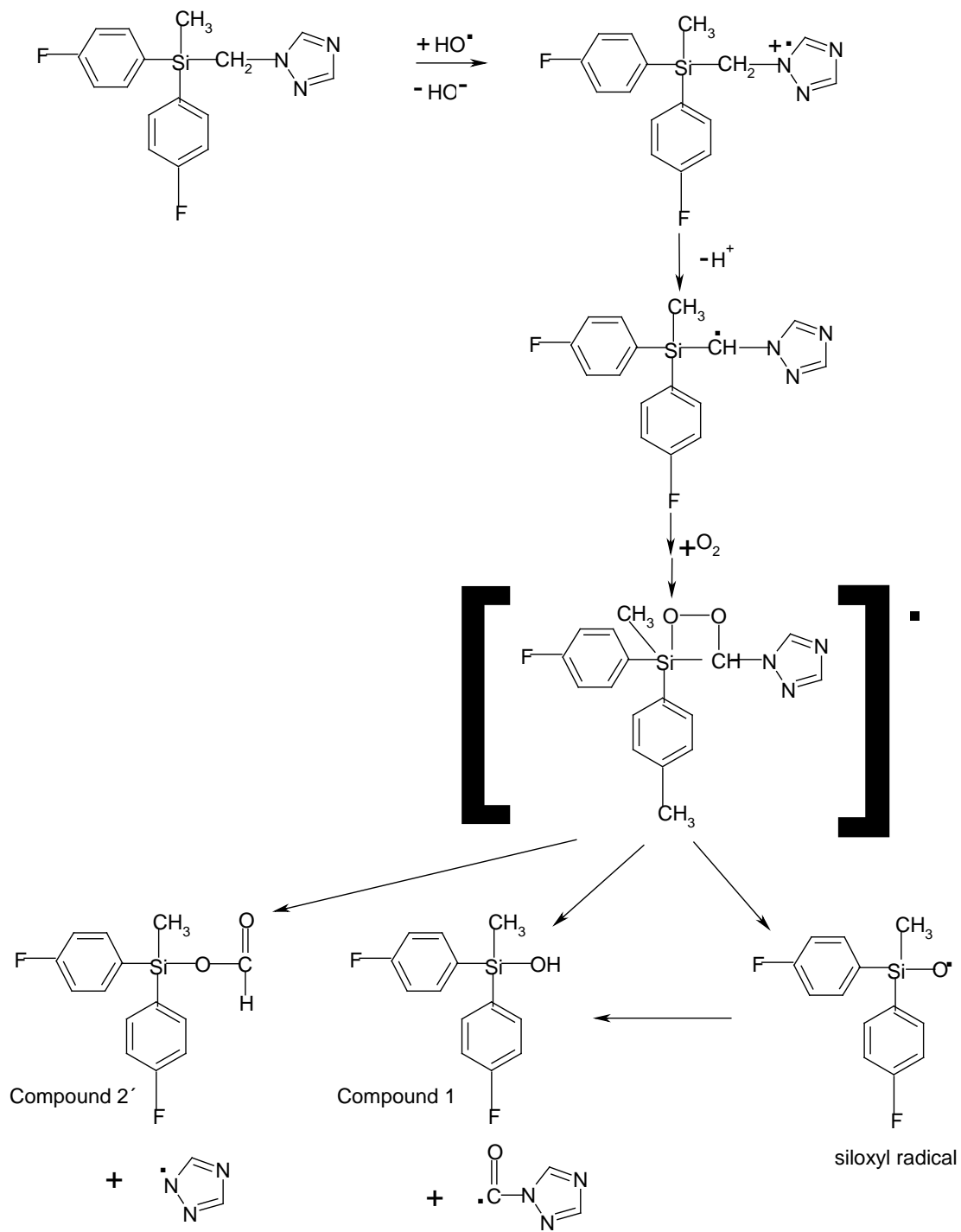
362

363

364   Scheme IV

365

366   The proposed mechanism is further supported by the fact that the rate constants reported for

367   these reactions are on the order of those found here for the reaction of HO$^\bullet$ with the fungicide

368   (Hiller and Asmus 1983) (Ross et al. 1998).

369   As shown in scheme IV, the proposed reaction mechanism might involve the formation of

370   silicon pentacoordinated intermediates after reaction of the α-aminoalkyl radical with

371   oxygen. This intermediate may explain the formation of identified products 1 and 2´. Besides,

372   compound 1 could be produced by hydrolysis of compound 2´ (Tuazon et al. 2000) or by

373   depletion of Si-O$^\bullet$ radical with an hydrogen donor, such as hydrogen peroxide. Siloxyl radical

374   intermediate could be proposed considering that the reaction mechanism with hydroxyl

375   radical is analog to that described of flusilazole with sulfate radical (see scheme II and III)

376   Disproportionation reaction of peroxyl radicals (scheme V), may lead to the formation of

377   hydroxyl and keto derivatives of flusilazole, neither of which was detected by GC-MS

378   spectroscopy. Compound 2 detected, is justified by hydroxyl radical attack on triazole ring

379   of keto derivatives of flusilazole, followed by hydrolysis.
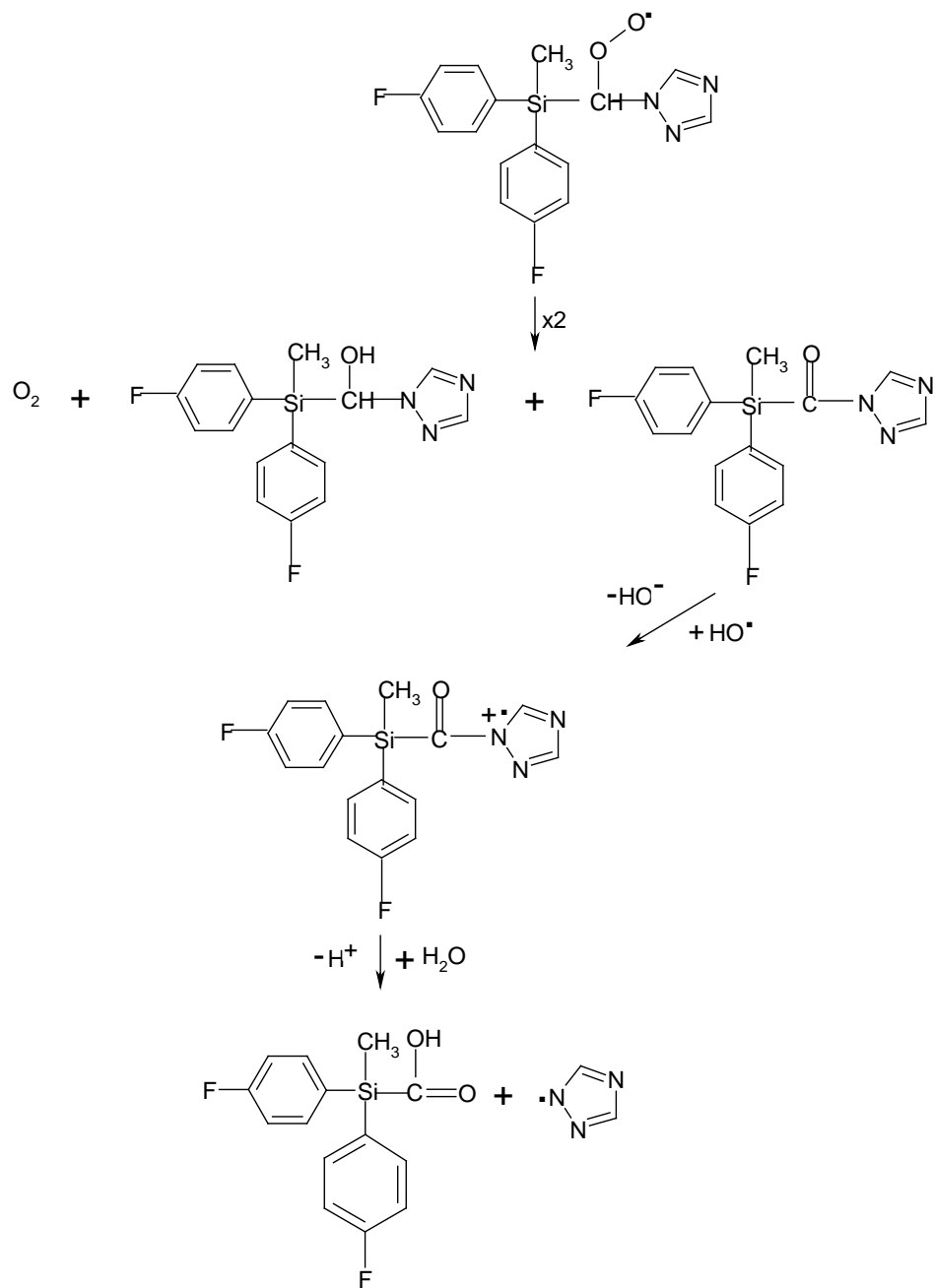
Compound 2

380

381

382   Scheme V

383

384   The observation that no nitrogen derivates were detected by GC-MS could be understood by

385   a fast rupture of silicon pentacoordinated intermediates followed by oxidation of the triazole

386   ring (Lhomme et al. 2007) (Guillard et al. 2002) (Le Campion et al. 1999).

387   Twenty minutes photo-fenton reaction with flusilazole leads to the formation of products

388   with higher molecular weight than flusilazole. GC-MS spectra for retention times > 28

389   minutes showed formation of compounds containing Si-O-C and Si-O-Si groups, such as

390   silicic acid, diethyl bis(trimethylsilyl) ester. The main route to obtain siloxane functional

391   group is by condensation of two silanols like those formed in the first minute's fenton

392   reaction, as showed in scheme III. Besides, molecules containing Si-O-C groups are proposed

393   to be generated as by-product in the same scheme (compound 2′). Silicic acid, diethyl

394   bis(trimethylsilyl) ester has no fluorine content in its structure. It indicates that between ten

395   and twenty minutes of photo-Fenton process, loss of fluoride starts taking place.

396   GC-MS peaks of $R_t < 26.5$ min are not easy identified in 20 minutes reaction. This might be

397   because the reaction system is too complex to recognize low molecular weight by-products.

398   Amat et al. (2009) described a similar complex system were a great number of low molecular

399   weight CG-MS products generated by fast cleavage of molecules, which did not allow the

400   elucidation of a detailed mechanism for the degradation of the chemicals.

401   In flusilazole metabolism in rats, goat, hens, apples, wheat, grapes and soil (Mastovska 2007)

402   (T. R. Roberts and Hutson 1990) and in environmental fate studies of the insecticide, the

403   main degradation product detected was [Bis(4-fluorophenyl)methyl] silanol ($C_{13}H_{12}F_2OSi$)

404   of molecular weight 250g/mol. Other polar metabolites containing silanol groups were

405   detected in the tissue residues and excretion samples analyzed in rats, goats, and hens.

406   Silicic acid, diethyl bis(trimethylsilyl) ester is a non toxic compound that is found in root and

407   inner bark extract of some medicinally important plants against human pathogens with

408   antioxidant activity (Anjaneyulu Musini 2013) (Hosseinihashemi et al. 2015) (Kathirvel et

409   al. 2014).

410   This compound is detected in GC-MS spectrum after the photo Fenton degradation of

411   flusilazole, what suggests that degradation of that organosilicon fungicide by this process is

412   an important route of decomposition yielding non toxic by-products.

413   Cleavage between the silicon and the triazole ring to form the silanol is the major metabolic

414   route in plants, which may be further metabolized to the silane diols or to disiloxane

415   (Mastovska 2007). The results in twenty minutes photo fenton experiments showed that a

416   siloxane (a silane ether) is produced, in line with the reported metabolic route.

417

418   Conclusions

419   The fungicide flusilazole chemically react with hydroxyl radical and sulfate radical anion

420   with rate constants of 2.0×10^9 s^{-1} M^{-1} and 4.6×10^8 s^{-1} M^{-1}, respectively.

421   Both reactions involve a charge transfer from the fungicide to the radicals, characteristic for

422   tertiary amines. Proton elimination from the ethyl carbon vecinal to the triazole N atom yields

423   α-aminoalkyl radicals detected as the main transients formed. The absorption spectra of the

424   transients observed in the range 300–700 nm could be assigned to carbon centered radicals

425   and siloxyl radicals in accordance to the DFT calculated spectra and with data reported by

426   Dell´Arciprete et al. (2011). The amidine nitrogen of the molecule is the preferred site of

427   attack by HO$^{•}$ and SO$_4^{•-}$ radicals.

428   In the degradation process, the presence of the element silicon in the fungicide compound is

429   essential to generate the intermediates proposed in the reaction path. The by-products

430   identified, could further yield silicates as the final product of degradation.

431

References

Anjaneyulu Musini, M. Jayaram Prakash Rao and Archana Giri. 2013. "Phytochemical Investigations and Antibacterial Activity of Salacia Oblonga Wall Ethanolic Extract." *Annals of Phytomedicine* 2 (1): 102–7.

Arce, Valeria B., Sonia G. Bertolotti, Fernando J. V. E. Oliveira, Claudio Airoldi, Antonio Arques, Lucas Santos-Juanes, Mónica C. Gonzalez, Carlos J. Cobos, Patricia E. Allegretti, and Daniel O. Mártire. 2012. "Triplet State of 4-Methoxybenzyl Alcohol Chemisorbed on Silica Nanoparticles." *Photochemical & Photobiological Sciences* 11 (6): 1032. doi:10.1039/c2pp05370e.

Baciocchi, Enrico, Tiziana Del Giacco, and Andrea Lapi. 2004. "Oxygenation of Benzyldimethylamine by Singlet Oxygen. Products and Mechanism." *Organic Letters* 6 (25). American Chemical Society: 4791–94. doi:10.1021/ol047876l.

Barone, Vincenzo, and Maurizio Cossi. 2001. "Conductor Solvent Model." *J. Phys. Chem. A* 102 (97): 1995–2001.

Bosio, Gabriela, Susana Criado, Walter Massad, Felipe J Rodríguez Nieto, Mónica C Gonzalez, Norman A García, and Daniel O Mártire. 2005. "Kinetics of the Interaction of

456   Sulfate and Hydrogen Phosphate Radicals with Small Peptides of Glycine, Alanine,

457   Tyrosine and Tryptophan." *Photochemical & Photobiological Sciences : Official Journal of*

458   *the European Photochemistry Association and the European Society for Photobiology* 4

459   (10). The Royal Society of Chemistry: 840–46. doi:10.1039/b507856c.

460   Buxton, George V., Clive L. Greenstock, W. Phillips Helman, and Alberta B. Ross. 1988.

461   "Critical Review of Rate Constants for Reactions of Hydrated Electrons, Hydrogen Atoms

462   and Hydroxyl Radicals (???OH/???O??? In Aqueous Solution." *Journal of Physical and*

463   *Chemical Reference Data* 17 (2): 513–886. doi:10.1063/1.555805.

464   Buxton, George V., Clive L. Greenstock, W. Phillips Helman, Alberta B. Ross, and Wing

465   Tsang. 1988. "Critical Review of Rate Constants for Reactions of Hydrated

466   electronsChemical Kinetic Data Base for Combustion Chemistry. Part 3: Propane." *Journal*

467   *of Physical and Chemical Reference Data* 17 (2). AIP Publishing: 513–886.

468   doi:10.1063/1.555805.

469   Carra, Irene, José Antonio Sánchez Pérez, Sixto Malato, Olivier Autin, Bruce Jefferson,

470   and Peter Jarvis. 2016. "Performance of Different Advanced Oxidation Processes for

471   Tertiary Wastewater Treatment to Remove the Pesticide Acetamiprid." *Journal of*

472   *Chemical Technology and Biotechnology* 91 (1): 72–81. doi:10.1002/jctb.4577.

473   Choure, S. C., M. M. M. Bamatraf, B. S. M. Rao, Ranjan Das, H. Mohan, and J. P. Mittal.

474   1997. "Hydroxylation of Chlorotoluenes and Cresols: A Pulse Radiolysis, Laser Flash

475   Photolysis, and Product Analysis Study." *The Journal of Physical Chemistry A* 101 (51).

476   American Chemical Society: 9837–45. doi:10.1021/jp971986a.

477   Cobos, Carlos J, and Adela E Croce. 2010. "Of the CF 3 OSO 3 Radical," 720–24.

478   Corriu, R. J. P, B. J. L Guerin, Henner, and Q Wang. 1991. "Pentacoordinate Intermediates

479   in the Hydrolysis Reaction of Organic Silicates." *Organometallics* 10 (4): 3200–3205.

480 doi:10.1021/om00055a042.

481 Criquet, Justine, and Nathalie Karpel Vel Leitner. 2009. "Degradation of Acetic Acid with

482 Sulfate Radical Generated by Persulfate Ions Photolysis." *Chemosphere* 77 (2). Elsevier

483 Ltd: 194–200. doi:10.1016/j.chemosphere.2009.07.040.

484 Das, S, and C von Sonntag. 1986. "The Oxidation of Trimethylamine by OH Radicals in

485 Aqueous Solution, as Studied by Pulse Radiolysis, ESR, and Product Analysis."

486 Dell'arciprete, María L, Carlos J Cobos, Jorge P Furlong, Daniel O Mártire, and Mónica C

487 Gonzalez. 2007. "Reactions of Sulphate Radicals with Substituted Pyridines: A Structure-

488 Reactivity Correlation Analysis." *Chemphyschem : A European Journal of Chemical*

489 *Physics and Physical Chemistry* 8 (17): 2498–2505. doi:10.1002/cphc.200700456.

490 Dell 'Arciprete, María L, Lucas Santos-Juanes, Antonio Arques Sanz, Rafael Vicente, Ana

491 M Amat, Jorge P Furlong, Daniel O Mártire, and Monica C Gonzalez. 2009. "Reactivity of

492 Hydroxyl Radicals with Neonicotinoid Insecticides: Mechanism and Changes in Toxicity."

493 *Photochem. Photobiol. Sci.* 8 (7): 1016–23.

494 Dell 'Arciprete, Mariá L, Carlos J Cobos, Daniel O Matire, Jorge P Furlong, and Monica C

495 Gonzalez. 2011. "Reaction Kinetics and Mechanisms of Neonicotinoid Pesticides with

496 Sulfate Radicals." *New J. Chem.* 35: 672–80. doi:10.1039/c0nj00726a.

497 Dimopoulou, Myrto, Aart Verhoef, Bennard van Ravenzwaay, Ivonne M C M Rietjens, and

498 Aldert H. Piersma. 2016. "Flusilazole Induces Spatio-Temporal Expression Patterns of

499 Retinoic Acid-, Differentiation- and Sterol Biosynthesis-Related Genes in the Rat Whole

500 Embryo Culture." *Reproductive Toxicology* 64. Elsevier Inc.: 77–85.

501 doi:10.1016/j.reprotox.2016.04.003.

502 Farag, A.T.; Ibrahim, H.H. 2007. "Developmental Toxic Effects of Antifungal

503 FlusilazoleAdmin Istered by Gavage to Mice." *Birth Defects Research (Part B)* 80: 12–17.

504 Faust, Bruce C., and Jürg Hoigné. 1990. "Photolysis of Fe (III)-Hydroxy Complexes as

505 Sources of OH Radicals in Clouds, Fog and Rain." *Atmospheric Environment Part A,*

506 *General Topics* 24 (1): 79–89. doi:10.1016/0960-1686(90)90443-Q.

507 Frisch, M. J.; Trucks, G. W.; Schlegel, H. B.; Scuseria, G. E.; Robb, M. A.; Cheeseman, J.

508 R.; Scalmani, G.; Barone, V.; Mennucci, B.; Petersson, G. A. 2009. "No Title."

509 GONZALEZ, Monica C., Daniel O. MARTIRE, and André M. BRAUN. 1998. "Aqueous

510 Phase Kinetic Studies Involving Highly Reactive Species of Environmental Interest."

511 *Recent Research Developments in Photochemistry and Photobiology* 2: 25–45.

512 http://cat.inist.fr/?aModele=afficheN&cpsidt=14194233.

513 Griessbach, E. F C, and R. G. Lehmann. 1999. "Degradation of Polydimethylsiloxane

514 Fluids in the Environment - A Review." *Chemosphere* 38 (6): 1461–68.

515 doi:10.1016/S0045-6535(98)00548-7.

516 Guillard, C., S. Horikoshi, N. Watanabe, H. Hidaka, and P. Pichat. 2002. "Photocatalytic

517 Degradation Mechanism for Heterocyclic Derivatives of Triazolidine and Triazole."

518 *Journal of Photochemistry and Photobiology A: Chemistry* 149 (1–3): 155–68.

519 doi:10.1016/S1010-6030(01)00653-0.

520 Hasegawa, Eietsu, Wei Xu, Patrick S Mariano, and Jin-uk Kim. 1988. "Eietsu Hasegawa,?

521 Wei Xu,? Patrick S. Mariano,*,? Ung-Chan," no. 6.

522 Hiller, K. O., and K. D. Asmus. 1983. "Formation and Reduction Reactions of .alpha.-

523 Amino Radicals Derived from Methionine and Its Derivatives in Aqueous Solutions." *The*

524 *Journal of Physical Chemistry* 87 (19). American Chemical Society: 3682–88.

525 doi:10.1021/j100242a022.

526 Hosseinihashemi, Seyyed Khalil, Hamidreza Anooshei, Hamed Aghajani, and Mohamed Z

527 M Salem. 2015. "Chemical Composition and Antioxidant Activity of Extracts from the

528 Inner Bark of Berberis Vulgaris Stem." *BioResources* 10 (4): 7958–69.

529 doi:10.15376/biores.10.4.7958-7969.

530 Ito, Takeo, Shota Morimoto, Shin ichi Fujita, and Sei ichi Nishimoto. 2009. "Radical

531 Intermediates Generated in the Reactions of L-Arginine with Hydroxyl Radical and Sulfate

532 Radical Anion: A Pulse Radiolysis Study." *Radiation Physics and Chemistry* 78 (4): 256–

533 60. doi:10.1016/j.radphyschem.2009.01.005.

534 Kathirvel, A., A. K. Rai, G. S. Maurya, and V. Sujatha. 2014. "Dryopteris Cochleata

535 Rhizome: A Nutritional Source of Essential Elements, Phytochemicals, Antioxidants and

536 Antimicrobials." *International Journal of Pharmacy and Pharmaceutical Sciences* 6

537 (SUPPL. 2): 179–88.

538 Kim, Soo-Myung, and Alfons Vogelpohl. 1998. "Degradation of Organic Pollutants by the

539 Photo-Fenton-Process." *Chemical Engineering & Technology* 21 (Ii): 187–91.

540 doi:10.1002/(SICI)1521-4125(199802)21:2<187::AID-CEAT187>3.0.CO;2-H.

541 Kozicki, Marek, Katarzyna Filipczak, and Janusz Marian Rosiak. 2003. "Reactions of

542 Hydroxyl Radicals, H Atoms and Hydrated Electrons with N,N′-Methylenebisacrylamide in

543 Aqueous Solution. A Pulse Radiolysis Study." *Radiation Physics and Chemistry* 68 (5):

544 827–35. doi:10.1016/S0969-806X(03)00311-6.

545 Lalevée, J, B Graff, X Allonas, and J P Fouassier. 2007. "Aminoalkyl Radicals: Direct

546 Observation and Reactivity toward Oxygen, 2,2,6,6-Tetramethylpiperidine-N-Oxyl, and

547 Methyl Acrylate." *The Journal of Physical Chemistry. A* 111 (30). American Chemical

548 Society: 6991–98. doi:10.1021/jp071720w.

549 Le Campion, Laurence, Charles Giannotti, and Jamal Ouazzani. 1999. "Photocatalytic

550 Degradation of 5-Nitro-1,2,4-Triazol-3-One NTO in Aqueous Suspention of TiO2.

551 Comparison with Fenton Oxidation." *Chemosphere* 38 (7): 1561–70. doi:10.1016/S0045-

552   6535(98)00376-2.

553   Lhomme, Ludovic, Stephan Brosillon, and Dominique Wolbert. 2007. "Photocatalytic

554   Degradation of a Triazole Pesticide, Cyproconazole, in Water." *Journal of Photochemistry*

555   *and Photobiology A: Chemistry* 188 (1): 34–42. doi:10.1016/j.jphotochem.2006.11.015.

556   Luo, Shuang, Zongsu Wei, Dionysios D. Dionysiou, Richard Spinney, Wei-Ping Hu,

557   Liyuan Chai, Zhihui Yang, Tiantian Ye, and Ruiyang Xiao. 2017. "Mechanistic Insight into

558   Reactivity of Sulfate Radical with Aromatic Contaminants through Single-Electron

559   Transfer Pathway." *Chemical Engineering Journal* 327. Elsevier B.V.: 1056–65.

560   doi:10.1016/j.cej.2017.06.179.

561   Mastovska, Katerina. 2007. "Food and Agriculture Organization of the United Nations."

562   *Eastern Regional Research Center, Agricultural Research Service, USA.*

563   http://www.fao.org/fileadmin/templates/agphome/documents/Pests_Pesticides/JMPR/Evalu

564   ation07/Flusilazole.pdf.

565   Navarro, Simón, José Fenoll, Nuria Vela, Encarnación Ruiz, and Ginés Navarro. 2011.

566   "Removal of Ten Pesticides from Leaching Water at Pilot Plant Scale by Photo-Fenton

567   Treatment." *Chemical Engineering Journal* 167 (1): 42–49. doi:10.1016/j.cej.2010.11.105.

568   Neta, P., Robert E. Huie, and Alberta B. Ross. 1988. "Rate Constants for Reactions of

569   Inorganic Radicals in Aqueous Solution." *Journal of Physical and Chemical Reference*

570   *Data* 17 (3). AIP Publishing: 1027. doi:10.1063/1.555808.

571   Ozakca, Dilek Unal, and Hulya Silah. 2013. "Genotoxicity Effects of Flusilazole on the

572   Somatic Cells of Allium Cepa." *Pesticide Biochemistry and Physiology* 107 (1). Elsevier

573   Inc.: 38–43. doi:10.1016/j.pestbp.2013.05.001.

574   Padmaja, S., Z. B. Alfassi, P. Neta, and R. E. Huie. 1993. "Rate Constants for Reactions of

575   SO4????? Radicals in Acetonitrile." *International Journal of Chemical Kinetics* 25 (3):

576   193–98. doi:10.1002/kin.550250307.

577   Roberts, Terry R., and David H. Hutson. 1990. *Metabolic Pathways of Agrochemicals.*

578   *Part2: Insecticides and Fungicides*. Edited by Terry R.; Roberts and David H. Hutson. 1st

579   ed. Cambridge: Royal Society of Chemistry.

580   Ross,W. G. Mallard,W. P. Helman, G. V. Buxton, R. E. Huie, P. Neta. 1998. "No Title."

581   *NDRL-NIST Solution Kinetics Database, Ver. 3.0. Notre Dame Radiation Laboratory,*

582   *Notre Dame, IN, US and National Institute of Standards and Technology,*

583   *Gaithersburg,MD, US.* http://kinetics.nist.gov/solution/.

584   Rosso, Janina A, Paula Caregnato, Veronica C Mora, Monica C Gonzalez, and Daniel O

585   Martire. 2003. "Reactions of Phosphate Radicals with Monosubstituted Benzenes. A

586   Mechanistic Investigation." *Helvetica Chimica Acta* 86: 2509–24.

587   doi:10.1002/hlca.200390203.

588   Schmider, Hartmut L, and Axel D. Becke. 1998. "Optimized Density Functionals from the

589   Extended G2 Test Set." *Journal Of Chemical Physics* 108 (23): 9624–31.

590   doi:10.1063/1.476438.

591   Sumalekshmy, S., and K. R. Gopidas. 2005. "Reaction of Aromatic Amines with

592   Cu(ClO4)2 in Acetonitrile as a Facile Route to Amine Radical Cation Generation."

593   *Chemical Physics Letters* 413 (4–6): 294–99. doi:10.1016/j.cplett.2005.06.041.

594   Suresh Das and V. Suresh. 2001. "Electron-Transfer Reactions of Amines." In *Electron*

595   *Transfer in Chemistry*, edited by V. Balzani, Wiley-VCH, 379–456. New York.

596   T. L. Luke, H. Mohan, V. M. Manoj, P. Manoj, J. P. Mittal and C. T. Aravindakumar.

597   2003. "Reaction of Sulphate Radical Anion (SO.4-) with Hydroxy-and Methyl-Substituted

598   Pyrimidines: A Pulse Radiolysis Study." *Res. Chem. Intermed.* 29 (4): 379–391.

599   Trovó, Alam Gustavo, S. A S Melo, and R. F P Nogueira. 2008. "Photodegradation of the

600 Pharmaceuticals Amoxicillin, Bezafibrate and Paracetamol by the Photo-Fenton Process-

601 Application to Sewage Treatment Plant Effluent." *Journal of Photochemistry and*

602 *Photobiology A: Chemistry* 198 (2–3): 215–20. doi:10.1016/j.jphotochem.2008.03.011.

603 TUAZON, ERNESTO C., SARA M. ASCHMANN, and ATKINSON ROGER. 2000.

604 "Atmospheric Degradation of Volatile Methyl-Silicon Compounds." *Environ. Sci. Technol*

605 34: 1970–76.

606 Wang, Chi Wei, and Chenju Liang. 2014. "Oxidative Degradation of TMAH Solution with

607 UV Persulfate Activation." *Chemical Engineering Journal* 254. Elsevier B.V.: 472–78.

608 doi:10.1016/j.cej.2014.05.116.

609